Distinct Binding of Cholesterol and 5β-Cholestane-3α,7α,12α-triol to Cytochrome P450 27A1: Evidence from Modeling and Site-Directed Mutagenesis Studies†

Natalia Mast,‡ Dilyara Murtazina,‡ Hong Liu,‡ Sandra E. Graham,§ Ingemar Bjorkhem,|| James R. Halpert,‡ Julian Peterson,§ and Irina A. Pikuleva*,‡

Department of Pharmacology and Toxicology, University of Texas Medical Branch, Galveston, Texas 77555-1031, Department of Biochemistry, University of Texas Southwestern Medical Center, 5323 Harry Hines Boulevard, Dallas, Texas 75390-9038, and Department of Clinical Chemistry, Karolinska Institute, Huddinge Hospital, S-141 88, Huddinge, Sweden

Received December 29, 2005; Revised Manuscript Received February 19, 2006

ABSTRACT: Cytochrome P450 27A1 (P450 27A1 or CYP27A1) is an important enzyme that participates in different pathways of cholesterol degradation as well as in the activation of vitamin D_3. Several approaches were utilized to investigate how two physiological substrates, cholesterol and 5β-cholestane-3α,7α,12α-triol, interact with CYP27A1. The enzyme active site was first probed spectrally by assessing binding of the two substrates and five substrate analogues followed by computer modeling and site-directed mutagenesis. The computer models suggest that the spatial positions and orientations of cholesterol and 5β-cholestane-3α,7α,12α-triol are different in the enzyme active site. As a result, some of the active site residues interact with both substrates, although they are situated differently relative to each steroid, and some residues bind only one substrate. Mutation of the overlapping substrate-contact residues (W100, H103, T110, M301C, V367, I481, and V482) affected CYP27A1 binding and enzyme activity in a substrate-dependent manner and allowed identification of several important side chains. T110 is proposed to interact with the 12α-hydroxyl of 5β-cholestane-3α,7α,12α-triol, whereas V367 seems to be crucial for correct positioning of the cholesterol C26 methyl group and for regioselective hydroxylation of this substrate. Distinct binding of the CYP27A1 substrates may provide insight into why phenotypic manifestations of cerebrotendinous xanthomatosis, a disease associated with CYP27A1 deficiency, are so diverse.

Cytochrome P450 27A1 (P450 27A1 or CYP27A1[1]) is a sterol 27-hydroxylase, a ubiquitously expressed polyfunctional enzyme involved in the classical bile acid biosynthetic pathway in the liver, in the activation of vitamin D_3 in the kidney, and in initiation of the alternative bile acid biosynthetic pathway in other tissues (*1*−*6*). Steroids that are metabolized by CYP27A1 include 7α-hydroxy-4-cholesten-3-one, 5β-cholestane-3α,7α-diol, and 5β-cholestane-3α,7α,-12α-triol (the liver), vitamin D_3 and 25-hydroxyvitamin D_3 (the kidney), and cholesterol (all tissues where the enzyme is expressed). Deficiency of 27-hydroxylase activity as a result of mutations in the *CYP27A1* gene leads to abnormal accumulation of cholesterol and cholestanol (5α-saturated analogue of cholesterol) in multiple tissues and development of cerebrotendinous xanthomatosis (CTX), a disease manifested by a variety of phenotypes including osteoporosis and premature atherosclerosis (*7*−*10*). If untreated, cerebrotendinous xanthomatosis is a slowly progressive, lethal disease.

The present work examines how two physiological substrates, cholesterol and 5β-cholestane-3α,7α,12α-triol, bind in the CYP27A1 active site. In our previous studies showing that CYP27A1 activity is stimulated by phospholipids (PLs), we observed that the extent of stimulation of the enzyme activity depends on the substrate used and is more pronounced in the case of cholesterol hydroxylation than in the case of 5β-cholestane-3α,7α,12α-triol hydroxylation (*11*). A similar effect, substrate-dependent alteration of enzyme activity, was also observed by Dahlback-Sjorberg et al. when the noncompetitive inhibitor cyclosporin A was used (*12*). Cholesterol has a planar, three-dimensional structure and only one hydroxyl group in the steroid nucleus, the 3β-hydroxyl. 5β-Cholestane-3α,7α,12α-triol has a bend at the A/B ring junction and three hydroxyls, all in α-orientation (Figure 1). It is possible that the two steroids occupy different regions within the substrate pocket, such that when the P450 conformation is changed upon effector (PLs or noncompetitive inhibitor) binding, hydroxylation of one of the substrates is affected to a greater extent than hydroxylation of the other substrate. This hypothesis was tested in the present work by generating cholesterol- and 5β-cholestane-3α,7α,12α-triol-bound computer models of CYP27A1 and validating them by site-directed mutagenesis.

† These studies were supported by U.S. Public Health Service Grants GM62882 and AG024336 (to I.A.P.) and GM43479 (to J.P.), NIEHS Center Grant ES06676, the Howard Hughes Medical Institute 1999 Biomedical Research Support Program for Medical Schools, Grant 53000266, and grants from the Swedish Science Council and Heart Lung Foundation (to I.B.).

* To whom correspondence should be addressed. Tel: (409) 772-9657. Fax: (409) 772-9642, E-mail: irpikule@utmb.edu.

‡ University of Texas Medical Branch.

§ University of Texas Southwestern Medical Center.

|| Karolinska Institute, Huddinge Hospital.

[1] Abbreviations: P450 27A1 or CYP27A1, cytochrome P450 27A1; CTX, cerebrotendinous xanthomatosis; PLs, phospholipids; KP_i, potassium phosphate buffer; HPCD, 2-hydroxypropyl-β-cyclodextrin; *E. coli*, *Escherichia coli*.

10.1021/bi052654w CCC: $33.50
Published on Web 03/21/2006

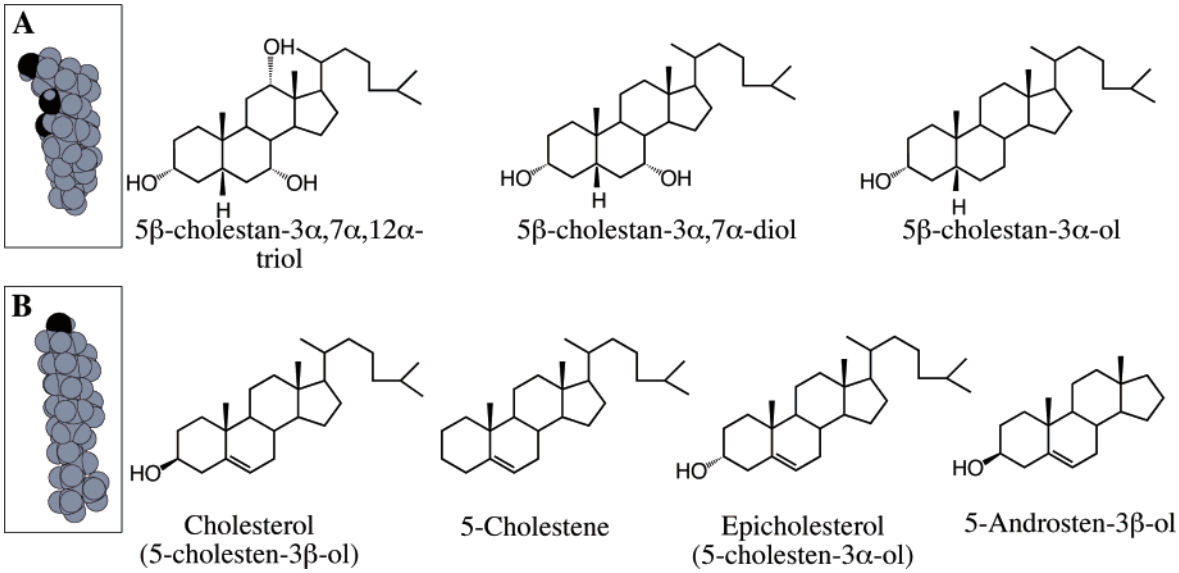

FIGURE 1: Chemical structures of compounds used in the present study. Insets A and B show space-filling models of 5*β*-cholestane-3α,7α,12α-triol and cholesterol, respectively. The models were generated by the program ChemBats3D Pro. Oxygen atoms are in black, and carbon atoms and hydrogens are in gray.

Table 1: Binding of Different Steroids to Wild Type CYP27A1

steroid	K_d, nM[a]	ΔA_{max}[b]
5*β*-cholestane-3α,7α,12α-triol	38 ± 12	0.037 ± 0.001
5*β*-cholestane-3α,7α-diol	132 ± 17	0.032 ± 0.006
5*β*-cholestan-3α-ol	220 ± 6	0.036 ± 0.002
5-cholesten-3*β*-ol (cholesterol)	26 ± 7	0.051 ± 0.006
5-cholestene	495 ± 73	0.016 ± 0.001
5-cholesten-3α-ol (epicholesterol)	32 ± 3	0.110 ± 0.003
5-androsten-3*β*-ol	186 ± 12	0.017 ± 0.001

[a] Calculated on the basis of the spectral binding as described under Experimental Procedures. The results represent the average of three different titrations ± SD. [b] Normalized to nmol of P450.

EXPERIMENTAL PROCEDURES

Substrate Docking. Substrates were docked in the previously constructed substrate-free model of CYP27A1 (the Protein Data Bank code 1MFX) (*13*) using InsightII modeling software (Molecular Simulations Inc., San Diego, CA). Structures of cholesterol and 5*β*-cholestane-3α,7α,12α-triol were generated and optimized by the Builder and Discover_3 programs of InsightII. The consistent valence force field was employed for energy minimization and molecular dynamics simulations of the substrate structures. Each of the substrates was then placed in the enzyme active site in an orientation allowing the production of (25*R*)-26-hydroxysteroid with the C26 atom placed 3.7 Å from the putative ferryl oxygen of the heme iron and one of the C26 hydrogens directed toward the iron so that the C−H−O angle was equal to 180°. The substrate-bound model was then energy minimized. During the minimization process, the amino acid side chains within 5 Å of the substrate were allowed to move. The substrate position was obtained in Discover_3 and the Docking program of InsightII using a consistent valence force field.

Site-Directed Mutagenesis. Mutations were introduced using an in vitro QuikChange site-directed mutagenesis kit (Stratagene) according to the instructions. The mutagenic oligonucleotides are shown in Table 1 of the Supporting Information. The correct generation of desired mutations and the absence of undesired mutations were confirmed by DNA sequencing of the entire CYP27A1 coding region.

Expression and Purification. The CYP27A1 wild type and mutants were expressed and partially purified as described (*11*). If the PL content of the enzyme preparation was higher than 6 μg/nmol of P450, an additional chromatography step was included. NaCl and Na cholate were added to the enzyme to a final concentration of 50 mM and 0.5%, respectively, and the solution was applied to a DEAE-cellulose column equilibrated with 50 mM potassium phosphate buffer (KP_i), pH 7.4, containing 20% glycerol, 50 mM NaCl, 0.5% Na cholate, and 1 mM EDTA. The flow-through fraction was collected, dialyzed against 40 mM KP_i, pH 7.4, containing 20% glycerol, and 1 mM EDTA, and used for substrate-binding and enzyme activity studies.

Spectral Binding Studies. The apparent binding constants (K_d) were determined as described (*14*). The P450 concentration was 0.3 μM in all experiments. Graph Prism software was used to calculate the K_d values by fitting spectral data in the quadratic equation that is applied when K_d is similar to or less than the enzyme concentration assuming 1:1 stoichiometry (*15*):

$$\Delta A = 0.5\Delta A_{max}(K_d + [E] + [S] - \sqrt{(K_d + [E] + [S])^2 - 4[E][S]})$$

where ΔA is the CYP27A1 spectral response at different substrate concentrations [S], ΔA_{max} is the maximal amplitude of the substrate-induced spectral response, and [E] is the enzyme concentration. After each experiment, the P450 content was quantified from the reduced CO-difference spectrum (*16*) to confirm the lack of enzyme denaturation. Titrations with 5*β*-cholestane-3α,7α,12α-triol, 5*β*-cholestane-3α,7α-diol, and 5*β*-cholestan-3α-ol were carried out at 18 °C in 50 mM KP_i, pH 7.4, containing 20% glycerol, and 1 mM EDTA. Steroid stocks (1 mM) were prepared in 2-hydroxypropyl-*β*-cyclodextrin (HPCD), using a minimal concentration of the vehicle (45%) required to dissolve the least soluble steroid 5*β*-cholestan-3α-ol. In studies evaluating

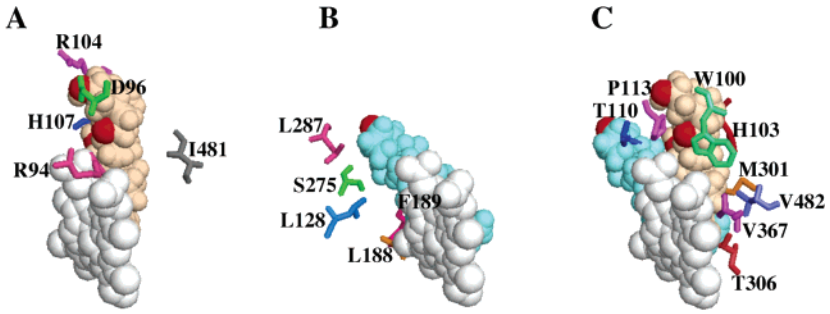

FIGURE 2: Models of the CYP27A1 active site in the complex with 5β-cholestane-3α,7α,12α-triol (A) and cholesterol (B) and when the two models are superimposed (C). 5β-Cholestane-3α,7α,12α-triol is in wheat, cholesterol is in cyan, heme is in light gray, and oxygen atoms in steroids are in red.

properties of the CYP27A1 mutants, ethanolic rather than HPCD solutions of 5β-cholestane-3α,7α,12α-triol were used. The K_d and ΔA_{max} values of CYP27A1 are essentially the same when the cholestane-3α,7α,12α-triol stock is made in ethanol instead of HPCD.

Cholesterol elicited a very weak spectral response in CYP27A1 in 50 mM KP_i, pH 7.4, containing 20% glycerol, and 1 mM EDTA, which necessitated modification of the assay conditions to yield reliable K_d values. By changing temperature, glycerol concentration, and ionic strength of the assay buffer, ΔA_{max} of the cholesterol-induced spin shift was increased 4-fold without any alteration of the K_d value. Similar results were obtained with cholesterol derivatives; therefore titrations with cholesterol, epicholesterol, 5-androsten-3β-ol, and 5-cholestene were conducted at 30 °C in 50 mM KP_i, pH 7.4, containing 10% glycerol, 0.5 M NaCl, and 1 mM EDTA. Stock solutions (0.25−0.5 mM) of the former three steroids were prepared in 4.5% HPCD, whereas 5-cholestene was dissolved in 45% HPCD because of its limited solubility in 4.5% HPCD at 0.25−0.5 mM concentrations. In a separate experiment we established that the concentration of HPCD in steroid stock (4.5% or 45%) does not change CYP27A1 affinity but does affect its ΔA_{max}, which is about 1.5-fold higher at 4.5% HPCD. For all studies, cholesterol stocks were prepared in 4.5% HPCD.

Enzyme Assays. Independent of the substrate used, the buffer was always 40 mM KP_i, pH 7.4, containing 1 mM EDTA, reaction volume 1 mL, and temperature 37 °C. Assay conditions were optimized for the formation of one product only, the 27-alcohol. Product formation was linear with time and enzyme concentration and did not exceed 21% of total substrate present. Reconstitution of 5β-cholestane-3α,7α,-12α-triol-hydroxylase activity was carried out using 0.01−0.3 μM P450, 0.05−1.5 μM adrenodoxin reductase (Adr), and 5 μM adrenodoxin (Adx) at two substrate concentrations: (1) a saturating concentration with both 30 μM 5β-cholestane-3α,7α,12α-triol and ~10 nM [^{3}H]5β-cholestane-3α,7α,12α-triol (80,000 cpm) and (2) a subsaturating concentration containing only the tritiated substrate (10 nM). The enzymatic reaction was initiated by addition of 1 mM NADPH and allowed to proceed for 1−3 min. Steroids were then extracted and analyzed as described (*17*). Reconstitution of cholesterol-hydroxylase activity required higher amounts of proteins and was carried out using 0.08−0.4 μM P450, 0.4−2.0 μM Adr, and 4−20 μM Adx. Two substrate concentrations were also used: a combination of 30 μM cholesterol and 2.2 nM [^{3}H]cholesterol (250 000 cpm), and 2.2 nM [^{3}H]cholesterol only. The reaction time was 4 min.

Other Methods. PL content in preparations of CYP27A1 wild type and mutants was estimated using ammonium ferrothiocyanate as described (*18*) following lipid extraction from 6 nmol of P450 with chloroform−methanol using the Blitch and Dyer method (*19*).

RESULTS

Interaction of Substrate Analogues with CYP27A1. Two groups of steroids were used: derivatives of 5β-cholestane-3α,7α,12α-triol and derivatives of cholesterol (Figure 1, Table 1). Titrations with 5β-cholestanes indicate that the 7α- and 12α-hydroxyls contribute moderately to steroid binding to CYP27A1. The K_d of 5β-cholestane-3α,7α-diol (lacks the 12α-hydroxyl) was 3.5-fold higher than that of 5β-cholestane-3α,7α,12α-triol, and the K_d of 5β-cholestan-3α-ol (lacks the 7α- and 12α-hydroxyls) was increased 5.7-fold. The two hydroxyls seem to be important for efficient catalysis because the rates of the product formation increase 2−5-fold as the number of hydroxyl groups increases, as established previously by others (*20*, *21*). The fact that the same position is hydroxylated in 5β-cholestan-3α-ol, 5β-cholestane-3α,7α-diol, and 5β-cholestane-3α,7α,12α-triol also suggests that the 7α- and 12α-hydroxyls are not essential for regioselectivity of hydroxylation of the 5β-cholestanes.

The role of cholesterol functionalities was ascertained by titration with the three derivatives. 5-Cholestene (lacks the 3β-hydroxyl) was found to have an almost 20-fold higher K_d than cholesterol, indicating a significant contribution of the 3β-hydroxyl to the strength of the complex formation with CYP27A1. Epicholesterol (differs from cholesterol by having the hydroxyl in the 3α position instead of the 3β position) had the same K_d as cholesterol, suggesting that the stereochemistry of the C3 hydroxyl is not important for steroid binding to the enzyme. Finally 5-androsten-3β-ol (lacks the side chain) yielded a 7-fold increase in K_d, implying that the side chain also plays a role in steroid interactions with CYP27A1.

Substrate-Bound Computer Models of CYP27A1. Two substrate-bound models were generated, one with 5β-cholestane-3α,7α,12α-triol, and the other one with cholesterol (Figure 2A,B). According to the models, the following amino acid residues lie within 5 Å from both substrates and are directed inside the enzyme active site or define the active site: W100, H103, T110, G112, P113, E298, M301, A302, T306, V367, and V482 (some of these residues are shown in Figure 2C). In addition, there is a set of residues that seem to interact with only one substrate (R94, D96, R104, H107,

and I481 with 5β-cholestane-3α,7α,12α-triol, and L128, L188, F189, S275, L287, and S295 with cholesterol) (Figure 2A,B). Superimposition of the two substrate-bound models shows that 5β-cholestane-3α,7α,12α-triol and cholesterol bind in a flipped orientation relative to each other, so that their α-atoms/groups (below the steroid plane) face each other and the β-atoms/groups (above the steroid plane) point in opposite directions. The spatial positions of the two substrates are also different except for the terminal portions of the steroid side chains, which partially overlap. Residues involved in contacts with only one substrate are located near the regions of the substrate molecules that are most separated spatially.

Mutagenesis Strategy. Only residues suggested to interact with both substrates were investigated to determine whether mutations differentially affect the binding and turnover of the two substrates. Conservative substitutions were made at 8 of 11 overlapping substrate-contact residues, each to a smaller and larger size side chain when possible. G112 and T306 were not mutated because they were already investigated by others (*22, 23*). A third residue, P113, was not studied because conservative substitutions of proline are not possible, and nonconservative substitutions are difficult to interpret unambiguously.

Mutations within the Putative Active Site. A total of 16 mutants were generated. Of them, W100F, E298D, and A302V resulted in the inactive P420 protein. No peak at 450 nm was detected in the reduced CO spectrum of the *Escherichia coli* (*E. coli*) cells expressing these mutants, although there was a strong immunoreactive signal on Western blots (not shown). Thirteen mutants did retain the P450 spectrum, and their properties are shown in Table 2, which also contains information about the PL content of each enzyme preparation. In our previous studies we established that contaminating PLs affect substrate binding and catalytic activity of CYP27A1 (*11*). Therefore comparison of a mutant P450 should be made to one of the three wild type preparations that has a similar PL content. Catalytic activity was measured at two substrate concentrations: (1) at saturating concentration when the rate of catalysis essentially represents the k_{cat} and (2) at a very low, subsaturating concentration, when the rate reflects catalytic efficiency (k_{cat}/K_m).

W100 defines the size of the active site in both models and is also close to one of the heme propionate groups. A smaller side chain at this position may adopt an orientation different from that of tryptophan and affect substrate binding and heme incorporation. Indeed, the W100L substitution weakened 5β-cholestane-3α,7α,12α-triol binding about 5-fold and abolished the cholesterol-induced spectral response. The latter could be due either to the lack of cholesterol binding or to the binding in an altered orientation that does not displace water from the heme iron. The W100L mutant was catalytically inactive with both substrates. Thus, 5β-cholestane-3α,7α,12α-triol either binds to CYP27A1 in an unproductive orientation or requires a hydrogen donor/acceptor at position 100 for efficient catalysis, or both.

H103 spatially constrains the steroid C18 methyl group in the 5β-cholestane-3α,7α,12α-triol-bound model and defines the size of the active site below steroid ring D in the cholesterol-bound model. Because of different space limitations, substitution with a larger side chain should have a greater impact on 5β-cholestane-3α,7α,12α-triol binding than on cholesterol binding. This prediction is in agreement with the properties of the H103F mutant, which had an increased K_d for 5β-cholestane-3α,7α,12α-triol and a decreased K_d for cholesterol (quantitative comparisons in the case of this mutant are not possible because of a lack of a wild type standard with a similar PL content). Significant contamination with PLs, despite repeated chromatography steps on DEAE-cellulose, precluded studies of the H103A mutant.

T110 interacts with the steroid 12α-hydroxyl in the 5β-cholestane-3α,7α,12α-triol-bound model and points below steroid ring A in the cholesterol-bound model. Replacement at this position with a non-hydrogen-bonding side chain should disrupt the CYP27A1 contacts with the 12α-hydroxyl and, consequently, have a more pronounced effect on enzyme interaction with 5β-cholestane-3α,7α,12α-triol than with cholesterol. The T110V mutation resulted in a 7.5-fold increase in the K_d for 5β-cholestane-3α,7α,12α-triol with no significant effect on cholesterol binding. Enzyme activity toward both substrates impaired to a similar extent at subsaturating substrate concentrations and to a greater extent with of 5β-cholestane-3α,7α,12α-triol when saturating concentrations of substrates were used. Conservative substitution with Ser weakened the affinity for 5β-cholestane-3α,7α,-12α-triol only 2-fold and even increased the affinity for cholesterol. The rates of 5β-cholestane-3α,7α,12α-triol hydroxylation were still decreased at both substrate concentrations, whereas the rates of cholesterol hydroxylation were the same as or even higher than those of the wild type at low and high substrate concentrations, respectively. Partial or full restoration of the two enzyme activities in the T110S mutant suggests that a hydrogen donor/acceptor group is required at position 110 for efficient catalysis.

M301 is located at the very top of the active site (the heme group forms the bottom) over the steroid C21 methyl group in the 5β-cholestane-3α,7α,12α-triol-bound model and almost perpendicular to the steroid side chain in the cholesterol-bound model. Because of a shorter distance to the 5β-cholestane-3α,7α,12α-triol C21 methyl than to the cholesterol side chain, M301 should play a lesser role in positioning of cholesterol than of 5β-cholestane-3α,7α,12α-triol. Mutations to a smaller Cys and to a larger Phe decreased CYP27A1 affinity for 5β-cholestane-3α,7α,12α-triol about 2-fold but enhanced cholesterol binding. Despite opposite effects on the affinity, the enzyme activity with both substrates was decreased.

V367 points toward the steroid C26 methyl group in both models. In the 5β-cholestane-3α,7α,12α-triol-bound model, V367 constrains this methyl group only, while in the cholesterol-bound model, V367 also defines the position of the C27 methyl. The V367 substitutions were expected to have a much more dramatic effect on cholesterol binding than on 5β-cholestane-3α,7α,12α-triol binding. Mutation to a smaller size Ala increased the K_d for 5β-cholestane-3α,7α,-12α-triol about 3-fold, a change consistent with elimination of a weak hydrophobic interaction, and abolished the cholesterol-induced spectral response. The rates of 5β-cholestane-3α,7α,12α-triol hydroxylation were reduced, whereas cholesterol hydroxylation was undetectable. Mutation to Leu had a minor effect on the interaction with both substrates and a more significant effect on the two enzyme activities, which were reduced. The V367L replacement

Table 2: Substrate Binding and Catalytic Properties of CYP27A1 Wild Type (WT) and Mutants[a]

		5β-cholestane-3α,7α,12α-triol					cholesterol				
		spectral assay		activity					activity		
P450	PL content, μg	K_d, nM	ΔA_{max} × 10^{-3}	product formation,[b] %	turnover,[c] min^{-1}	location in model	K_d, nM	ΔA_{max} × 10^{-3}	product formation,[b] %	turnover,[c] min^{-1}	location in model
WT	1.8	36 ± 9	57 ± 4	20.7 ± 3.8	68 ± 16		26 ± 7	51 ± 6	0.42 ± 0.10	3.0 ± 0.9	
WT	2.8	34 ± 5	45 ± ±8	nd[d]	≤68[e]		111 ± 5	44 ± 2	0.54 ± 0.08	2.0 ± 0.4	
WT	5.7	150 ± 20	45 ± 10	nd	≤68[e]		320 ± 80	10± ±	nd	nd	
						Mutations of the Putative Active Site Residues					
W100L	1.9	171 ± 4	15 ± 1	no activity[f]		defines the active site near steroid 7α-OH, may also play a role in heme stability	no spectral response[g]		no activity		defines the active site below steroid rings C and D, may also play a role in heme stability and
W100F		inactive P420 protein				and incorporation	inactive P420 protein				incorporation
H103A	30	nd				spatially constrains steroid	nd				defines the active site below
H103F	4.4	140 ± 20	13 ± 1	7.7 ± 0.4	17 ± 3	C18 methyl	31 ± 4	12 ± 1	0.28 ± 0.10	1.3 ± 0.1	steroid ring D
T110V	2.9	180 ± 40	37 ± 2	6.3 ± 0.7	11 ± 3	interacts with the steroid	44 ± 11	10 ± 1	0.12 ± 0.02	1.1 ± 0.3	points below steroid ring A
T110S	2.6	67 ± 14	31 ± 2	12.0 ± 0.2	24 ± 3	12α-OH	11 ± 3	18 ± 1	0.55 ± 0.12	4.0 ± 0.4	
E298D		inactive P420 protein				in the vicinity of the steroid 12α-OH	inactive P420 protein				defines active site below steroid ring D
M301C	<1	73 ± 12	26 ± 2	10.7 ± 1.4	35 ± 8	defines the active site above	2.6 ± 0.5	10 ± 2	0.13 ± 0.01	1.1 ± 0.2	defines the active site across steroid side chain
M301F	1.9	69 ± 2	44 ± 2	16.3 ± 3.1	15 ± 3	steroid C21 methyl	7 ± 2	7 ± 1	0.15 ± 0.03	1.0 ± 0.1	
A302V		inactive P420 protein				points inside the active site, involved in positioning of the steroid C27 methyl	inactive P420 protein				points inside the active site, involved in positioning of the steroid C27 methyl
V367A	2.6	107 ± 10	38 ± 2	2.9 ± 0.3	13 ± 1	points toward steroid	no spectral response		no activity		points toward steroid
V367L	2.5	61 ± 7	25 ± 2	6.6 ± 0.2	10 ± 1	C26 methyl	8±2	28(1	0.11 ± 0.03 + additional product	1.0 ± 0.2	C26 methyl
I481A	2.0	160±50	28±2	6.0±0.6	8±1	defines the active site near C20−	310±90	2(0.1	0.05±0.01	0.5±0.1	>5 Å from cholesterol side
I481V	2.0	31±13	36±7	5.3±0.1	8±1	C22 of the steroid side chain	4±1	21(1	0.35±0.04	2.6±0.2	chain
V482A	2.7	51±2	44±2	11.5±0.7	57±2	points inside the active site	33±1	10(2	0.06±0.01	0.5±0.1	points inside the active site
V482L		unstable protein				toward steroid C25	unstable protein				toward steroid C27 methyl
						Mutations of the Putative Non Active Site Residues					
M97C	3.4	970±90	14±3			points away from the active site	no spectral response		0.01 ± 0.001	no activity	points away from the active site
L109V	1.7	88 ± 16	37 ± 10			points away from the active site	16 ± 1	14 ± (1	0.24 ± 0.02	1.0 ± 0.3	points away from the active site
Y111C	2.0	118 ± 18	42 ± 4			points below the heme plane	4 ± 1	10 ± 3	0.14 ± 0.04	1.0 ± 0.1	points below the heme plane
Y111F	3.5	170 ± 40	28 ± 2				90 ± 23	15 ± 2	0.37 ± 0.08	3.0 ± 0.5	
F114L	17	nd					nd				
T115S		inactive P420 protein					inactive P420 protein				
W121F		inactive P420 protein				highly conserved across many P450s	inactive P420 protein				highly conserved across many P450s
L299I	2.8	29 ± 6	45 ± 10			points away from the active site	28 ± 3	54 ± 1	0.40± ± 0.11	1.8 ± 0.5	points away from the active site
L299V	2.6	52 ± 20	36 ± 1				14 ± 3	36 ± 1	0.28 ± 0.04	1.9 ± 0.2	
V304A	1.1	160 ± 20	49 ± 3			points away from the active site	5 ± 1	15± ± 1	0.28 ± 0.07	1.6 ± 0.4	points away from the active site
V304L	2.1	69 ± 28	24 ± 1			toward helix E	no spectral response		0.03 ± 0.01	0.2 ± 0.05	toward helix E
V366A	1.6	36 ± 2	44 ± 6			points toward the heme vinyl group,	5 ± 1	18 ± 1	0.2 ± 0.02	2.1 ± 0.3	points toward the heme vinyl group,
V366L		low level of expression				a larger side chain would destabilize the heme	low level of expression				a larger side chain would destabilize the heme
T369V	1.6	74 ± 13	42 ± 1			defines the active site but >5 Å from the steroid	32 ± 3.6	80 ± 2	0.52 ± 0.18	3.2 ± 0.6	defines the active site but >5 Å from the steroid
N370L	2.5	35 ± 16	37 ± 9			points inside the active site but >5	8 ± 3	23 ± 1	0.19 ± 0.02	1.6 ± 0.1	points inside the active site but >5
N370Q		inactive P420 protein				Å from the steroid	inactive P420 protein				Å from the steroid
S371A	2.7	51 ± 14	46 ± 2			points away from the active site	28 ± 3	52 ± 2	0.38 ± 0.07	2.2 ± 0.6	points away from the active site
S371V		low level of expression					low level of expression				
L483I	1.5	92 ± 30	27 ± 1			adjacent to and interacting with the I helix,	29 ± 6	7 ± 2	0.15 ± 0.05	1.2±0.1	adjacent to and interacting with the I helix,
L483V		unstable protein				changes would affect the I helix	unstable protein				changes would affect the I helix

[a] All results represent the average of 3−4 independent experiments ± SD. PL content and ΔA_{max} in the spectral binding assay are normalized to nmol of P450. [b] Measured at subsaturating substrate concentrations, normalized to time and nmol of P450. [c] Measured at saturating substrate concentration. [d] Not determined. [e] The turnover number of this preparation was not determined; from our previous studies (*11*) we know that at such concentrations *E. coli* PLs do not inhibit hydroxylation of 5β-cholestane-3α,7α,12α-triol. [f] No product formation was detected when enzyme concentration and reaction time were simultaneously increased, each 5-fold, compared with the enzyme concentration and reaction time used for the wild type assay. [g] The spectral response was <0.002 absorbance units when 2 μM P450 was titrated with up to a 100 μM steroid.

resulted in a loss of regioselectivity toward cholesterol, but not 5β-cholestane-3α,7α,12α-triol, as indicated by appearance of an additional peak in the cholesterol HPLC product profile. Thus, V367 appears to be essential for correct cholesterol docking as well as for regioselectivity of hydroxylation.

I481 defines the size of the active site near carbons C20−C24 of the steroid side chain in the 5β-cholestane-3α,7α,-12α-triol-bound model and is located >5 Å from the steroid in the cholesterol-bound model. Mutation to the significantly smaller Ala increased the K_d values for 5β-cholestane-3α,7α,12α-triol and cholesterol about 4- and 12-fold, respectively, and reduced both enzyme activities. The effect on cholesterol-binding was not predicted based on the model. A possible explanation is that this mutation led to a conformational change in the β4 turn where I481 is located and affected substrate interaction with the neighboring V482. The conservative I481V substitution did not decrease CYP27A1 affinity for either of the substrates but reduced the rates of 5β-cholestane-3α,7α,12α-triol hydroxylation.

V482 points inside the active site toward C25 of the steroid side chain in the 5β-cholestane-3α,7α,12α-triol-bound model and toward the steroid C27 methyl group in the cholesterol-bound model. Mutation to Ala only insignificantly (<1.5-fold) decreased 5β-cholestane-3α,7α,12α-triol binding and did not alter cholesterol binding. The rate of 5β-cholestane-3α,7α,12α-triol hydroxylation was decreased ~2-fold at a subsaturating substrate concentration but was similar to that of the wild type at a saturating substrate concentration. The rates of cholesterol hydroxylation were decreased to a greater extent, with a 9-fold decrease at low substrate concentration, and a 4-fold decrease at a high cholesterol concentration. V482L was unstable and could not be purified and characterized.

Mutations outside the Putative Active Site. Positions outside the vicinity of the putative active site residues were also mutated to test the models (Table 2). Enzyme activity was measured only with cholesterol, because radiolabeled 5β-cholestane-3α,7α,12α-triol is commercially unavailable and we had limited amounts of this substrate.

M97, which is located −3 and −6 residues, respectively, from the active site W100 and H103, points outside the active site. Smaller or larger substitutions at this position may affect W100 and H103, and exert an indirect effect on substrate binding. Indeed, M97C showed significantly weakened 5β-cholestane-3α,7α,12α-triol binding and yielded no cholesterol-induced spectral response and essentially no cholesterol hydroxylase activity.

L109 and Y111 flank the active site T110. L109 points away from the active site, whereas Y111 is directed below the heme plane near one of the heme propionates. Replacement of L109 should not have a significant effect on binding of either substrate. Substitution of Y111, however, may result in a different orientation of the side chain and affect neighboring T110 and consequently interaction with 5β-cholestane-3α,7α,12α-triol but not with cholesterol. As predicted by the models, the L109V mutation had only a minor effect on 5β-cholestane-3α,7α,12α-triol binding and no effect on cholesterol binding. The Y111 substitutions increased the K_d for 5β-cholestane-3α,7α,12α-triol 3.3−4.7-fold and had no effect on affinity for cholesterol. These changes were similar to those caused by the T110V substitution, raising an alternate interpretation of the data obtained, namely, that alignment and consequently the model in this loop region is not correct and that it is Y111 but not T110 that forms a hydrogen bond with the 12α-hydroxyl. Arguments against such interpretation are as follows. First, there is a very limited space around the 12α-hydroxyl of 5β-cholestane-3α,7α,12α-triol in the model permitting only a small side chain in the vicinity of this hydroxyl. T100 meets this requirement very well. Second, the T110S substitution significantly restored the 5β-cholestane-3α,7α,12α-triol binding, which also supports the suggested role of T110.

L299 and V304 reside in the putative helix I, which contains E289, A302, and M301, all of which are suggested to form part of the CYP27A1 active site. L299 and V304 both point away from the active site with the side chain of L299 having no spatial constraints and that of V304 defined by helix E. Accordingly, alterations in substrate binding may be observed upon replacement of V304 but not of L299. A smaller size substitution of V304 may alter the position of M301 located above the C21 methyl of 5β-cholestane-3α,7α,12α-triol and thus alter the interaction with this substrate, whereas cholesterol binding should not be affected. A larger substitution may cause a shift in the helix I by pushing it against the E helix and influence binding of cholesterol, which is located closer to this part of the helix than 5β-cholestane-3α,7α,12α-triol. The observed properties of the L299 and V304 mutants are in agreement with this prediction. The L299I and L299V mutants had unchanged K_d values for both substrates. The V304A mutant had a 4.4-fold increased K_d for 5β-cholestane-3α,7α,12α-triol, while affinity for cholesterol was not impaired. The V304L mutant had unaltered affinity for 5β-cholestane-3α,7α,12α-triol but showed no spectral response upon cholesterol binding.

Four residues, V366, T369, N370Q, and S371, were studied in the loop region that contains the active site V367. Position 368 was not mutated because it is occupied by proline. V366 and S371 point away from the active site, T369 defines the active site but is more than 5 Å from either of the substrates, and N370 points inside the active site but, like S369, is too far from 5β-cholestane-3α,7α,12α-triol and cholesterol. None of the replacements in this region, except V367, are expected to affect substrate binding. The V366, T369, N370Q, and S371 mutants had essentially unaltered affinities for both substrates and thus validated the models and the suggested role of V367.

L483 points outside the substrate pocket, flanking the active site V482, and interacts with the I helix. Substitutions of L483 may cause conformational changes in the I helix and affect substrate binding and/or protein stability. The L483I replacements resulted in a 2.5-fold increased K_d for 5β-cholestane-3α,7α,12α-triol and no impairment of the affinity for cholesterol. The L483V mutation produced unstable protein, which precluded further studies.

DISCUSSION

The goal of the present study was to compare how cholesterol and 5β-cholestane-3α,7α,12α-triol, the two important physiological substrates of CYP27A1, bind in the enzyme active site. A combination of computer modeling and site-directed mutagenesis was utilized. It was possible to dock each of the substrates in only one reactive orientation

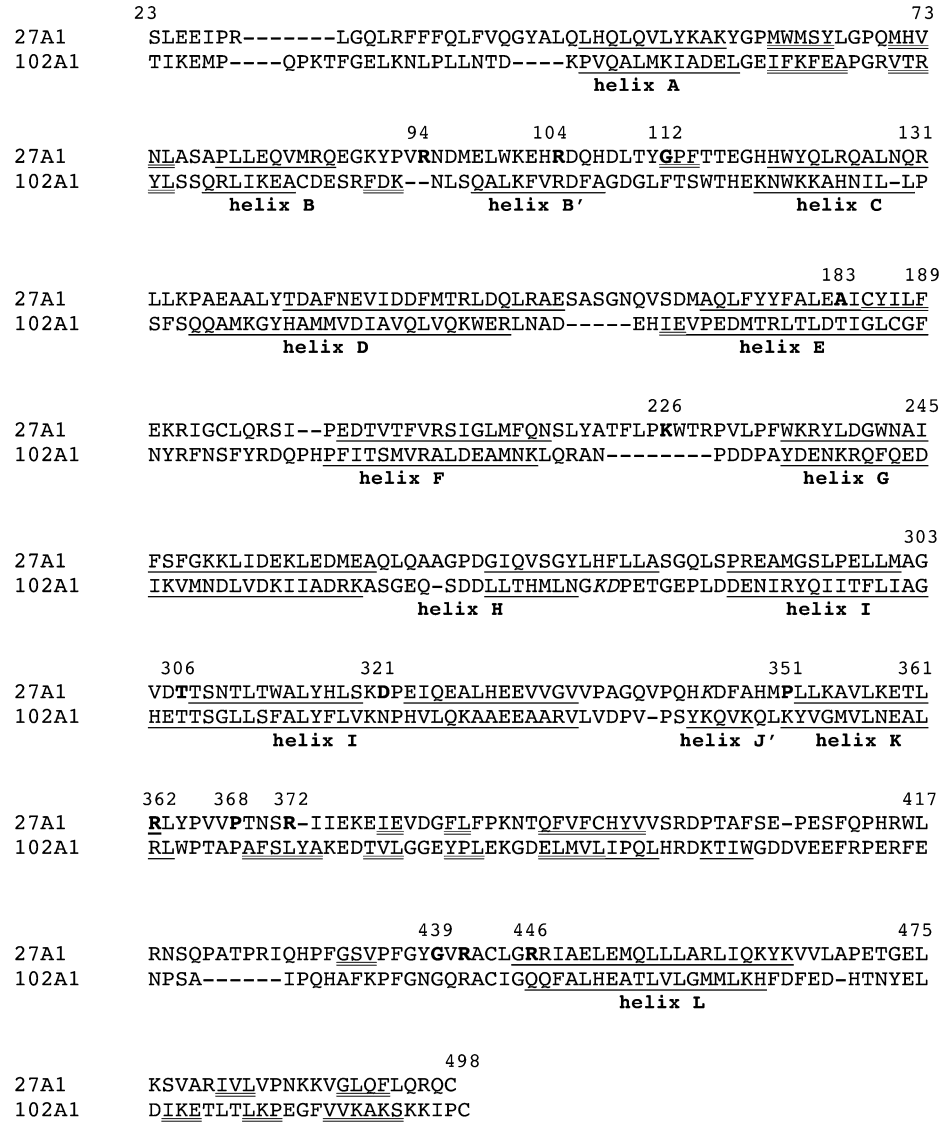

FIGURE 3: Alignment of CYP27A1 with CYP102A1 (PDB code 1FAG) used for modeling. α-Helices and *β*-strands are underlined with single and double lines, respectively. These secondary structural elements of CYP27A1 were predicted using the program JPRED, and those of CYP102A1 were taken from the PDB structure 1FAG. Residues whose mutations cause CTX are in bold.

in the CYP27A1 active site, with the resulting spatial positions of their steroid nuclei being significantly different and only the positions of the carbons C25 and C26 similar. Residues identified by the models to be involved in the interaction with each of the substrates were found to partially overlap. The overlapping substrate-contact residues were mutated. Most of these mutations (W100L, H103F, T110V, T110S, M301C, M301F, V367A, and V367L) had differential effects on binding of the two substrates studied. This result was consistent with the modeling data suggesting that cholesterol and 5*β*-cholestane-3α,7α,12α-triol occupy different regions within the substrate-binding pocket and bind in different orientations. Replacements of the putative non active site residues located in the vicinity of the suggested active site residues were also carried out. The observed effects were all well explained by the models and provided further support for the models regarding the role of T110 and V367.

We were also interested in identification of the group in the enzyme active site that forms a hydrogen bond with the cholesterol 3*β*-hydroxyl, because titrations with 5-cholestene suggested that this functionality is important for cholesterol interaction with CYP27A1. No side chain was found in the vicinity of the cholesterol 3*β*-hydroxyl in the model; there was only one contact with the oxygen from the peptide bond formed by the residues E291 and A292. The role of the 3α-hydroxyl of 5*β*-cholestane-3α,7α,12α-triol was not ascertained in the present work, but by analogy with cholesterol, it is reasonable to assume that this hydroxyl may also be important for binding to CYP27A1. In the model, the 3α-hydroxyl is surrounded by D96, R104, and the oxygen from the G112−P113 peptide bond. The four residues are located in the region (positions 94−115, Figure 3) that contains 16 side chains with hydrogen-bonding capacity that likely form a network stabilizing the P450 structure. Substitutions of the residues in this region (R94K, W100F, and T115S) often produce an improperly folded protein [ref *23* and the present work]. Therefore it was decided not to replace D96 and R104.

Knowledge that alterations of the CYP27A1 properties are substrate-dependent is of dual importance. First, the results may have pharmacological relevance and should be taken into account when evaluating side effects of drugs that noncompetitively inhibit CYP27A1. These drugs may have differential effects on cholesterol turnover through the

classical and alternative bile acid biosynthetic pathways as well as on vitamin D_3 production. Second, the present work contributes to our understanding of why clinical symptoms are so diverse in CTX patients. Thus far, 20 missense mutations (mutations that resulted in amino acid replacement) encompassing 14 amino acid residues have been found to underlie CTX (*9*, *10*, *24*) (Figure 3). Five of these residues are conserved in the P450 superfamily and are known to be important for heme binding and protein folding (*25*). Their substitutions (R94Q, R94W, R362C, R362Q, R362H, R362S, R372Q, R372W, G439A, R441Q, R441W) most likely produce nonfunctional enzyme and abolish all enzymatic activities. Biochemical consequences of the other missense mutations such as R104W, G112E, A183P, K226R, T306M, D321G, P351L, P368R, and R446C are not so obvious. In our previous in vitro studies, the K226R CTX mutation was reproduced (*13*). This mutant was able to hydroxylate cholesterol, although at a 4.5-fold reduced catalytic efficiency, demonstrating that an enzyme that is still catalytically active can be produced as a result of a missense mutation. The present investigation suggests that different missense mutations may lead to different disease manifestations because of the differential effects on the numerous enzyme activities. Many steroids serve as physiological substrates for CYP27A1. It should no longer be assumed that disruption of enzyme activity toward one substrate leads to a simultaneous disruption of the enzyme activities toward all substrates. Several enzyme activities should be measured when characterizing CTX patients. The data may help to reveal genotype−phenotype correlations at least in the case of some missense mutations.

In summary, previous studies of Dahlback-Sjoberg et al. were the first to suggest that 5β-cholestane-3α,7α,12α-triol and cholesterol have different orientations in the CYP27A1 active site (*12*). A similar conclusion was then drawn in our investigation focused on the role of PLs in CYP27A1 function (*11*). Finally, distinct binding of the two substrates was supported by the present work which through molecular modeling and site-directed mutagenesis provided concrete information about regions and residues in CYP27A1 that are likely involved in the interaction with cholesterol and 5β-cholestane-3α,7α,12α-triol. The present work is the first comprehensive investigation of the CYP27A1 active site that may also contribute to clarification of the mechanisms underlying phenotypic heterogeneity associated with CTX.

ACKNOWLEDGMENT

Oligonucleotide synthesis and DNA sequencing were carried out by the recombinant DNA Laboratory and the Protein Chemistry Laboratory, respectively, at the University of Texas Medical Branch.

SUPPORTING INFORMATION AVAILABLE

One table listing oligonucleotides used to generate CYP27A1 mutants. This material is available free of charge via the Internet at http://pubs.acs.org.

REFERENCES

1. Wikvall, K. (1984) Hydroxylations in biosynthesis of bile acids. Isolation of a cytochrome P-450 from rabbit liver mitochondria catalyzing 26-hydroxylation of C27-steroids, *J. Biol. Chem. 259*, 3800−3804.
2. Okuda, K., Masumoto, O., and Ohyama, Y. (1988) Purification and characterization of 5 beta-cholestane-3 alpha,7 alpha,12 alpha-triol 27-hydroxylase from female rat liver mitochondria, *J. Biol. Chem. 263*, 18138−18142.
3. Usui, E., Noshiro, M., Ohyama, Y., and Okuda, K. (1990) Unique property of liver mitochondrial P450 to catalyze the two physiologically important reactions involved in both cholesterol catabolism and vitamin D activation, *FEBS Lett. 274*, 175−177.
4. Vlahcevic, Z. R., Stravitz, R. T., Heuman, D. M., Hylemon, P. B., and Pandak, W. M. (1997) Quantitative estimation of the contribution of different bile acid pathways to total bile acid synthesis in the rat, *Gastroenterology 113*, 1949−1957.
5. Lund, E., Andersson, O., Zhang, J., Babiker, A., Ahlborg, G., Diczfalusy, U., Einarsson, K., Sjovall, J., and Bjorkhem, I. (1996) Importance of a novel oxidative mechanism for elimination of intracellular cholesterol in humans, *Arterioscler., Thromb., Vasc. Biol. 16*, 208−212.
6. Norlin, M., von Bahr, S., Bjorkhem, I., and Wikvall, K. (2003) On the substrate specificity of human CYP27A1: implications for bile acid and cholestanol formation, *J. Lipid Res. 44*, 1515−1522.
7. Cali, J. J., Hsieh, C. L., Francke, U., and Russell, D. W. (1991) Mutations in the bile acid biosynthetic enzyme sterol 27-hydroxylase underlie cerebrotendinous xanthomatosis, *J. Biol. Chem. 266*, 7779−7783.
8. Bjorkhem, I., and Leitersdorf, E. (2000) Sterol 27-hydroxylase defficiency: a rare cause of xanthomas in normocholesterolemic humans, *Trends Endocrinol. Metab. 11*, 180−183.
9. Verrips, A., Hoefsloot, L. H., Steenbergen, G. C., Theelen, J. P., Wevers, R. A., Gabreels, F. J., van Engelen, B. G., and van den Heuvel, L. P. (2000) Clinical and molecular genetic characteristics of patients with cerebrotendinous xanthomatosis, *Brain 123* (Part 5), 908−919.
10. Lee, M.-H., Hazard, S., Carpten, J. D., Yi, S., Cohen, J., Gerhardt, G. T., Salen, G., and Patel, S. B. (2001) Fine-mapping, mutational analyses, and structural mapping of cerebrotendinous xanthomatosis in U.S. pedigrees, *J. Lipid Res. 42*, 159−169.
11. Murtazina, D. A., Andersson, U., Hahn, I. S., Bjorkhem, I., Ansari, G. A., and Pikuleva, I. A. (2004) Phospholipids modify substrate binding and enzyme activity of human cytochrome P450 27A1, *J. Lipid Res. 45*, 2345−2353.
12. Dahlback-Sjoberg, H., Bjorkhem, I., and Princen, H. M. (1993) Selective inhibition of mitochondrial 27-hydroxylation of bile acid intermediates and 25-hydroxylation of vitamin D3 by cyclosporin A, *Biochem. J. 293* (Part 1), 203−206.
13. Murtazina, D., Puchkaev, A. V., Schein, C. H., Oezguen, N., Braun, W., Nanavati, A., and Pikuleva, I. A. (2002) Membrane-protein interactions contribute to efficient 27-hydroxylation of cholesterol by mitochondrial cytochrome P450 27A1, *J. Biol. Chem. 277*, 37582−37589.
14. Mast, N., and Pikuleva, I. A. (2005) A simple and rapid method to measure cholesterol binding to P450s and other proteins, *J. Lipid Res. 46*, 1561−1568.
15. Copeland, R. A. (2000) Protein−ligand binding equilibria, in *Enzymes* (Copeland, R. A., Ed.) 2nd ed., pp 76−108, A John Wiley & Sons, Inc., New York.
16. Omura, R., and Sato, R. (1964) The carbon monoxide-binding pigment of liver microsomes, *J. Biol. Chem. 239*, 2370−2378.
17. Pikuleva, I. A., Babiker, A., Waterman, M. R., and Bjorkhem, I. (1998) Activities of recombinant human cytochrome P450c27 (CYP27) which produce intermediates of alternative bile acid biosynthetic pathways, *J. Biol. Chem. 273*, 18153−18160.
18. Stewart, J. C. (1980) Colorimetric determination of phospholipids with ammonium ferrothiocyanate, *Anal. Biochem. 104*, 10−14.
19. Johnson, A. R. (1971) Extraction and purification of Lipids, in *Biochemistry and Methodology of Lipids* (Johnson, A. R., and Davenport, J. B., Eds.), pp 131−136, John Wiley & Sons, Inc., New York.
20. Atsuta, Y., and Okuda, K. (1982) Partial purification and characterization of 5β-cholestane-3α,7α,12α-triol and 5β-cholestane-3α,7α-diol 27-monoozygenase, *J. Lipid Res. 23*, 345−351.
21. Ohyama, Y., Masumoto, O., Usui, E., and Okuda, K. (1991) Multifunctional property of rat liver mitochondrial cytochrome P-450, *J. Biochem. 109*, 389−393.
22. Reshef, A., Meiner, V., Berginer, V., and Leitersdorf, E. (1994) Molecular genetics of cerebrotendinous xanthomatosis in Jews of North African origin, *J. Lipid Res. 35*, 478−483.

23. Sawata, N., Sakaki, T., Kitanaka, S., Kato, S., and Inouye, K. (2001) Structure-function analysis of CYP27B1 and CYP27A1. Studies on mutants from patients with vitamin D-dependent rickets type I (VDDR-I) and cerebrotendinous xanthomatosis, *Eur. J. Biochem. 268*, 6607−6615.
24. Lamon-Fava, S., Schaefer, E. J., Garuti, R., Salen, G., and Calandra, S. (2002) Two novel mutations in the sterol 27-hydroxylase gene causing cerebrotendinous xanthomatosis, *Clin. Genet. 61*, 185−191.
25. Peterson, J. A., and Graham, S. E. (1998) A close family resemblance: the importance of structure in understanding cytochromes P450, *Structure 6*, 1079−1085.

BI052654W